Kinetics of Perfluorooctanoic and Perfluorooctane Sulfonic Acid Biodegradation by *Acidimicrobium* sp. Strain A6 during the Feammox Process

Matthew W. Sima, Shan Huang, and Peter R. Jaffé*

Department of Civil and Environmental Engineering, Princeton University, Princeton, NJ 08544, USA.

*Corresponding Author Jaffe@Princeton.edu

Abstract

Per- and polyfluoroalkyl substances (PFAS) are emerging contaminants of concern due to their health effects and persistence in the environment. Although perfluoroalkyl acids (PFAAs), such as perfluorooctanoic acid (PFOA) and perfluorooctanesulfonic acid (PFOS) are very difficult to biodegrade because they are completely saturated with fluorine, it has recently been shown that *Acidimicrobium* Sp. A6 (A6), which oxidizes ammonium under iron reducing conditions (Feammox process), can defluorinate PFAAs. A kinetic model was developed and tested in this study using laboratory batch incubation experiments to couple the Feammox process to PFAS defluorination. The experimental results show higher Feammox activity and PFAS degradation in A6 enrichment cultures than in pure A6 cultures. The coupled experimental and modeling results show that the PFAS defluorination rate is proportional to the rate of ammonium oxidation. The ammonium oxidation rate and the defluorination rate increase monotonically, but not linearly, with increasing A6 biomass. Given that different batches of A6 cultures have different level of Feammox activity, the parameters required to simulate the Feammox experiments varied between A6 batches, whereas parameters required to link the Feammox process to PFAS defluorination remained relatively constant between A6 batches.

Keywords: Feammox, *Acidimicrobium* sp. Strain A6, kinetic modeling, defluorination, PFAS.

Environmental Implication

There is significant concern about the widespread presence of per and polyfluorinated alkyl substances (PFAS) in the environment given their associated health concerns. Perfluorinated compounds are extremely recalcitrant and have been dubbed "forever chemicals". It has recently been shown that Acidimicrobium sp. Strain A6 (A6), an anaerobic ammonium oxidizer, is capable of defluorinating perfluorinated compounds such as PFOA and PFOS. This research focuses on linking the kinetics of this defluorination process with the rate of ammonium oxidation by A6 and the A6 biomass, providing new insights into the factors that drive this defluorination in systems favoring the growth of A6.

1. Introduction

Perfluorooctanoic Acid (PFOA) and Perfluorooctane Sulfonate (PFOS) are the two most studied and regulated per- and polyfluoroalkyl substances (PFAS) (Kucharzyk et al., 2017; Naidu et al., 2020; Teaf et al., 2019; USEPA, 2020). Degradation of PFOA and PFOS under natural conditions is difficult, especially compared to their precursors (e.g., fluorotelomers), because their non-functional carbons contain only the C-C and the very strong C-F but no C-H bonds (Buck et al., 2011; Liu and Avendano, 2013; Sima and Jaffé, 2020; Naidu et al., 2020). Compared to physical and chemical remediation methods, biological degradation may be more cost-effective, despite its slow defluorination rate (Ahmed et al., 2020; Naidu et al., 2020; Bolan et al., 2021; Liu and Avendano, 2013). Under natural soil-water environmental conditions, PFAS may be transformed or degraded into different shorter chain PFAS or into PFAS with different functional groups (e.g., carboxylic acid and phosphate esters), all of which are primarily mediated by microbial activity (Allred et al., 2015; Liu and Liu, 2016; Hamid et al., 2018). In fact, it is much more common for a particular PFAS to be transformed into shorter carbon chain products or those with different functional groups via chemical (e.g., hydrolysis) and biological (aerobic and anaerobic) reactions (Liu and Liu, 2016, Che et al. 2021), than to be fully degraded to its inorganic components (e.g., CO_2, SO_4^{2-}, and F^-) (Huang and Jaffé, 2019).

Many microbes such as *P. plecoglossicida* (Chetverikov et al., 2017), *P. parafulva* (Yi et al., 2016), and *P. aeruginosa* (Kwon et al., 2014) are capable of partially degrading PFAS (Bolan et al., 2021; Liu and Avendano, 2013). Beskoski et al. (2018) also showed that chemoorganoheterotrophic bacteria, as well as yeast and molds, could reduce PFOA and PFOS moderately. Apart from the bacterial composition, environmental factors (pH, Eh, and chemical composition) are also important to determine the optimal degradation rate of PFAS compounds

(Bolan et al., 2021). In general, bacteria diversity was adversely affected by the presence of PFAS, but some microbes were shown to thrive in PFAS contaminated soils (Senevirathna et al., 2022; Ji et al., 2021). For example, Senevirathna et al. (2022) showed a higher microbial population of *Alphaproteobacteria*, *Acidobacteria*, and *Gammaproteobacteria* in PFAS contaminated soils than in the surrounding non-contaminated soils.

Recently, Huang and Jaffé (2019) showed that PFOA and PFOS are degradable in anaerobic incubations during the Feammox process (ammonium oxidation under iron reduction) by *Acidimicrobium* sp. Strain A6 (referred to as A6 from here on), including in biosolids augmented with A6 and ferrihydrite (Huang et al., 2022), as well as in bioelectrochemical reactors (Ruiz et al., 2022), where the anode is the electron acceptor instead of ferric iron. A6 is an autotroph that thrives in iron rich acidic soils (Huang et al., 2016), which was isolated and grown as a pure culture by Huang and Jaffé (2018). The Feammox reaction, when ferrihydrite is the ferric iron source, is written as (Huang and Jaffé, 2018):

$$3Fe_2O_3{\bullet}0.5H_2O + 10H^+ + NH_4^+ \rightarrow 6Fe^{2+} + 8.5H_2O + NO_2^- \quad (1)$$

Results from 100-day incubation experiments (Huang and Jaffé, 2019) showed that PFOA degraded faster than PFOS, and that incubations with an A6 enrichment culture, as opposed to a pure A6 culture, resulted in higher PFAS defluorination rates. Furthermore. incubations with A6 enrichment cultures, vs. incubations with pure or relatively pure A6 cultures, resulted in the production of higher amounts of shorter carbon chain intermediate PFAS byproducts (PFBA, PFPeA, PFHxA, and PFHpA from PFOA and PFBS and PFBA from PFOS), indicating a synergy among microbes present in the enrichment culture and multiple possible defluorination mechanisms. Similar results were also found by Ruiz et al. (2022) using bioelectrochemical reactors seeded with A6. Results by Huang and Jaffé (2019) also showed that

the fraction of PFOA and PFOS that was defluorinated over a specific time was independent of the initial PFAS concentration, which varied over 3 orders of magnitude, indicating, that at least over the studied concentration range, a first order kinetic with respect to the concentration of the PFAS compounds is appropriate to describe such defluorination kinetics. It was also shown that PFAS degradation, at the concentrations studied, had little or no effects on the Feammox process in terms of NH_4^+ oxidized (Huang and Jaffé, 2019). It has been hypothesized by Huang and Jaffé (2019) that A6 can defluorinated PFAS, but being an autotroph, it is unable to break the carbon-carbon bonds, thus, other heterotrophs present in the enrichment culture will break the carbon-carbon bond once the carbon atom is no longer fully saturated with fluorine. While the A6 enrichment cultures usually contain about 40% A6 by bacterial numbers, it is exceedingly difficult to maintain an absolutely pure culture for long term incubations. Many "pure" A6 cultures for which A6 numbers and total bacterial numbers were the same at t = 0, have exhibited an A6 purity after a month or two of incubation of about 90% or higher. In such "pure A6 culture" incubations, minor amounts of intermediates have also been detected (Ruiz et al., 2021). Hence, in this manuscript, the pure A6 culture will refer to an A6 culture with upwards of 90% purity at the end of the incubations, to differentiate it from the A6 enrichment culture which has an A6 purity of at most 40% and a much higher presence of various heterotrophs throughout the whole incubation period (Huang and Jaffé, 2019).

The objectives of this study were to gain further insights into the kinetics of PFOA defluorination by A6 and to develop a simple kinetic model to describe the coupled Feammox/PFAS defluorination processes. This will be based on results from the study by Huang and Jaffé (2019) and augmented via incorporation of further experiments that focus on the effect of A6 biomass on the degradation rate of PFOA, as well as longer-term experiments where

NH_4^+ ,Fe(III), and CO_2 are replenished, pH adjusted, and some Fe(II) withdrawn at different times during the incubation (Jaffé et al., 2021). Insights gained from this effort will aid in assessing PFAS dynamics at locations where the Feammox process is occurring naturally, and/or for an eventual design of an A6-based bioremediation process.

2. Materials and Methods

The study consisted of three different sets of experiments, conducted at different times, as well as supplemental datasets that were used to test the models derived from the three primary experiments. The goal of the first set of experiments hereafter denoted as Experiment 1 was to investigate PFOA degradation at different initial PFOA concentrations (0.1, 10, and 100 mg/L) at the same initial A6 concentration. The goal of the second set of experiments, denoted as Experiment 2, was to study PFOA degradation (100 mg/L) at different initial A6 concentrations. The third set of experiments, denoted as Experiment 3, which was not used for modeling purposes, was designed to study PFOA degradation at a consistent high Feammox reaction rate by replenishing the medium with highly concentrated NH_4^+ and Fe(III) solutions at 15-day intervals to demonstrate the effect of maintaining more ideal growth conditions on the long-term reaction rates. The various experiments, and their use in model calibration and testing, which is described below, is illustrated in Figure 1.

2.1 PFOA degradation for different initial PFOA concentrations (Experiment 1)

To focus on the defluorination kinetics as a function of the initial PFOA concentrations, experimental results from Huang and Jaffé (2019) as well as results from additional incubations described below were used.

For all incubations, two hundred milliliters of either a pure A6 culture or an A6 enrichment culture, obtained from a Feammox laboratory-scale continuous-flow membrane reactor, which has been operated for 180 days, were mixed with 500 mL of an anoxic inorganic Fe(III)−NH_4^+ enrichment medium. This medium consisted of 7.5 mM 6-line ferrihydrite ($Fe_2O_3 \cdot 0.5H_2O$ prepared according to Cornell and Schwertmann, 2003), 2.81 mM NH_4Cl, 0.19 mM $(NH_4)_2SO_4$, 0.24 mM $NaHCO_3$, 0.71 mM $KHCO_3$, 0.07 mM KH_2PO_4, 0.41 mM $MgSO_4 \cdot 7H_2O$, and 0.40 mM $CaCl_2 \cdot 2H_2O$, in addition to 1 mL/L of a trace element solution and 1 mL/L of a vitamin solution (ATCC MD-VS). The mixture of medium and culture was then shaken in an anaerobic chamber for 24 h prior to the incubations. An electron shuttling compound necessary for the growth of the pure A6 strain (Huang and Jaffe, 2018), 9,10-anthraquinone-2,7-disulphonic acid (AQDS), was added to the pure A6 culture to yield a concentration of 25 μM. These mixtures were evenly distributed into multiple 10 mL serum vials in an anaerobic chamber and sealed with butyl rubber stoppers. The headspace (3 mL) of each vial was vacuumed and then flushed with a N_2/CO_2 (80:20) mixture to achieve anoxic conditions and provide additional CO_2 to the vials for A6 growth. All steps for the inoculation and isolation were carried out under sterilized conditions (autoclaved vials, and the media filtered through a 0.2 μm membrane). The Eh in the vials was −135 ±17 mV, and the initial pH was 4.5 ± 0.2 and increased to 5.0 ±0.2 during the incubations.

Incubations as described above were conducted by Huang and Jaffé (2109), and augmented for this research, with initial concentrations of 0.24 μM, 24 μM, and 0.24 mM PFOA, and 0.20 μM, 20 μM, and 0.20 mM PFOS (equivalent to 0.1 mg/L, 10 mg/L, and 100 mg/L of PFOA/PFOS). The higher PFOA/PFOS concentrations compared to what is typically found at

contaminated sites was selected to allow for more accurate F^- analyses, and to possibly evaluate the effect of defluorination on the reduction of Fe(III). For each set of experiments, several controls were prepared, including a positive control that was identical to those described above but without PFOA/PFOS to compare the Feammox activity in the absence of PFAS. All vials were placed on a rotary shaker at 150 rpm at ambient temperature for the incubations. On days 0, 7, 35, 60, and 100, three vials were destructively sampled for Fe(II), NH_4^+, PFOA/PFOS, F^-, shorter carbon-chain intermediates, and microbial analyses (A6) as described in detail in Huang and Jaffé, 2019.

An additional set of incubations with 3 mM of NH_4^+ and 12 mM of Fe(III) was conducted for initial PFOA concentrations of 24 μM (10 mg/L) and sampled at 0, 7, 25, and 60 days. 16S, along with microbial analysis, and concentrations of NH_4^+, F^- and PFOA were monitored for this set of incubations, while Fe(II) was not measured. This experiment was conducted at a different time, using a different batch of A6 with different Feammox activity, than the 100 mg/L and 0.1 mg/L experiments (Fig. 1), which will be accounted for in the analyses described below.

2.2 PFOA degradation at different initial A6 concentrations (Experiment 2)

Either the pure A6 culture or the A6 enrichment culture, both of which had been acclimated to PFOA for 3 months, were mixed with an anoxic inorganic Fe(III)−NH_4^+ medium, to prepare batch incubations with initial A6 concentrations of $1.0x10^4$, $1.0x10^5$, $1.0x10^6$, and $1.0x10^7$ copies/mL using the method described in Huang and Jaffé (2018). Then, PFOA was added to the vials, to yield an initial concentration of 0.24 mM (100 mg/L). Incubation vials were prepared and conducted for 30 days at 25°C as described above. Autoclaved controls and controls without PFOA

were run in parallel. Triplicate samples were collected destructively for Fe(II), NH_4^+, and PFOA analyses on day 0, 5, 15, and 30, and A6 biomass was measured for day 0.

2.3 PFOA degradation during NH_4^+ and ferrihydrite replenishment experiments (Experiment 3):

During batch incubations, the Feammox reaction as well as the defluorination reaction slowed down over time, possibly due to the depletion of NH_4^+, Fe(III), and/or CO_2, increase in pH, and/or buildup of reaction products such as Fe(II). Therefore, an longer-term experiment was set up in which a fraction of the vial's total volume was regularly removed, thus removing some of the Fe(II) that had accumulated, while also replenishing the vials with NH_4^+ and Fe(III) back to its initial volume and decreasing the pH from 6/6.5 to 4.5 using HCl. This resulted in a dilution of PFOA and F^- at each replenishment step, which is considered in the analyses. The goal of this experiment was to study the effect of this replenishment, and corresponding enhanced Feammox activity, on PFOA degradation by A6 over longer incubation periods. PFOA at an initial concentration of 0.24 mM was incubated in 100 mL vials with an incubation volume of 50 mL. A 2.5 mL sample was removed from each vial on days 0, 15, 30, 45, 60, 75, 90, 105, and 120 to conduct the routine chemical and microbiological analyses. On days 30, 60, and 90, a total of 5 mL of a solution containing 18 mM NH_4^+ and 12 mM Fe(III) was added to replace the solution withdrawn and replenish the oxidized NH_4^+ and reduced Fe(III). Measurements of NH_4^+, PFOA, and F^- were conducted at each of these timepoints. The initial A6 concentration for this experiment was 10^6 copies/mL (Fig. 1).

2.4 Coupled kinetics between PFOA defluorination and Feammox process considering the A6 biomass for the Feammox process and for defluorination

For the kinetic formulation presented here, the Feammox process is assumed to follow a first-order kinetic with respect to the NH_4^+ concentration. In the formulation it is assumed that the defluorination rate of PFOA/PFOS is proportional to the NH_4^+ oxidation since that is the source of electrons for the reduction of both Fe(III) and PFAS. Since the concentration of Fe(III) is orders of magnitude higher than that of PFOA, it is assumed that the defluorination of PFOA does not impact the reduction of Fe(III) in a measurable manner, although it was shown by Huang and Jaffé that when PFOA/PFOS is 100 mg/l there is a measurable decrease in Fe(III) reduction when either of these compounds is defluorinated. It is further assumed that the growth rate of A6 is proportional to the oxidation rate of NH_4^+, since NH_4^+ is the energy source for the growth of A6. In terms of biomass, based on the results from the defluorination experiments for different initial A6 biomass (Experiment 2), it is assumed that the Feammox and defluorination kinetics are both proportional but not linearly dependent to the A6 biomass. Based on the results of the incubations with different initial A6 biomass (Fig S1 and Fig S2), the reaction rates for NH_4^+ oxidation and PFAS reduction are considered to be a power function of the microbial biomass, rather than the more typical first order rate with respect to the biomass (Abhijith and Ostfeld, 2021; Murray et al., 2019; and Starzak, 1994). Thus, the following system of equations for the coupled Feammox/PFOA defluorination process was formulated:

$$\frac{dC_{NH4}}{dt} = -k_{NH4} C_{FeIII} C_{A6}^{1/n} C_{NH4} \quad (2)$$

$$\frac{dC_{FeIII}}{dt} = -k_{FeIII} C_{NH4} C_{A6}^{1/n} C_{FeIII} \quad (3)$$

$$\frac{dC_{PFOA}}{dt} = -f_{PFOA} k_{NH4} C_{FeIII} C_{NH4} C_{A6}^{1/m} C_{PFOA} \quad (4)$$

$$\frac{dC_F}{dt} = f_F \left[-\frac{dC_{PFOA}}{dt} \right] \quad (5)$$

$$\frac{dC_{A6}}{dt} = f_{A6}\left[-\frac{dC_{NH4}}{dt}\right] - k_d C_{A6} \quad (6)$$

Where C_{NH4}, C_{FeIII}, C_{PFOA}, and C_F are concentrations of NH_4^+, Fe(III), PFOA, F^-, in solution (mg/L), respectively. C_{A6} is the A6 concentration, measured and expressed as the A6 16S rRNA gene concentration, and k_{NH4} and k_{FeIII} are the oxidation rate constant of NH_4^+ and reduction rate constant of Fe(III), respectively (both with a derived unit of (L^(1+1/n)/(10*copies^(1/n)*mg*hr). The fractions (dimensionless) of NH_4^+ oxidized used for PFOA defluorination, F^- production, and A6 growth are f_{PFOA}, f_F, and f_{A6}, respectively. The A6 endogenous decay rate is k_d, which is assumed to be negligible over the timeframe of the simulations in this study. The exponents, m and n, are used to describe the non-linear dependence of PFOA degradation rate and Feammox activity (NH_4^+ oxidation/Fe(III) reduction rates) to the A6 concentration (see discussion below and results shown in Figs. S1 and S2).

Note that the shorter carbon chain PFAAs, that are produced during the degradation of PFOA or PFOS as shown by of Huang and Jaffé (2019) and Ruiz et al. (2022), are not included in this formulation. The incubations by Huang and Jaffé (2019) showed that these smaller PFAAs that were produced during these incubations, could contain up to 16% of the total fluorine initially present in the PFOA added, which is not considered directly in the formulation shown by Equation 5 and will require further fine tuning in subsequent model formulations requiring detailed insights into the degradation kinetics of these smaller carbon-chain PFAAs.

2.6 Numerical solution and parameter optimization

The system of equations shown above was solved using the finite difference method and the parameters (k_{NH4}, k_{FeIII}, f_{PFOA}, f_F, f_{A6}) were fitted to the Feammox and PFOA degradation data simultaneously using the Levenberg-Marquartdt algorithm (Simunek et al., 2012; Kool et al.,

1987). Specifically: (1) For a given (or initial) value (β_i) for each of the parameters, based on the initial concentrations of PFOA, NH_4^+, Fe(III), and A6 [$C_i(t=0)$], calculate the concentration change $\Delta C_i(t)$ at Δt (=0.5 h) by applying the finite difference method to Equations (2-6). (2) Update the concentrations at $t+\Delta t$, $C_i(t+\Delta t)= C_i(t)+ \Delta C_i(t)$ and continue the time steps until t=T (end of the experiment). (3) Iterate through all the chemicals in Equations (2-6) until a new $C_i(t+\Delta t)$ is found that satisfies all the Equations (2-6). (4) For parameter optimization, the simulated C_i's for each chemical at time $t=t_1, t_2, \ldots, t_n$ (n is number of sampling time) are compared to the experimental measurements (y_i) and the sum of squared errors ($SSE=\sum(y_i-C_i)^2$) is calculated for all chemicals and sampling times. (5) If the SSE (Sum Squared Error) does not meet a certain preset criterion, a Jacobian matrix (J) is calculated from simulated C_i's at β_i and C_i's at $\beta_i + 0.01\beta_i$. (6) A new parameter set $\beta = \beta + \Delta\beta$ is then calculated from the Jacobian matrix, where the increment $\Delta\beta = (J^TJ)^{-1}J^T[Y-C(\beta)]$ with Y and $C(\beta)$ as observed and simulated arrays of concentrations for all chemicals and sample times. (7) Iterate the above optimization procedure for all the chemicals until the SSE reaches a preset criterion. A schematic of the model is shown in Figure S3.

2.7 Model parameterization and evaluation

The results from the experiments described above were then used for the model calibration and testing. A schematic on how the datasets were utilized for this purpose is shown in Figure 1.

The model formulation and experimental results were used to: (1) Derive the exponents, m and n, in conjunction with NH_4^+ and PFOA kinetic data from the experiment with initial different A6 numbers (Experiment 2); (2) Derive the parameters, k_{NH4}, k_{FeIII}, and f_{A6}, by

calibrating the model to the pure Feammox reaction without PFOA. The value of f_{A6} that was obtained via this calibration, was then used for all other PFAS experiments, assuming that A6 growth is not affected by the presence of PFAS (Huang and Jaffé, 2019); (3) Derive the parameters, k_{NH4}, k_{FeIII}, f_F, and f_{PFOA} by fitting the model to the initial PFOA degradation experiments (Experiment 1) for an initial PFOA concentration of 100 mg/L; (4) Test if the model could predict the Feammox process and PFOA defluorination for the experiments with different initial PFOA concentrations using the parameters obtained from step (3).

Further testing of the model for a companion dataset of PFOS was conducted by fitting the 100 mg/L PFOS Feammox/PFOS defluorination data and predicting the 10 mg/L and 0.1 mg/L PFOS incubation data (Table 1 and Fig. 1).

3. Results and Discussion

3.1 Experimental Results

3.1.1 Feammox Activity and PFOA Degradation as a Function of initial PFOA Concentration (Experiment 1)

Concentrations of NH_4^+, PFOA, and F^- in solution for the experiments with an initial A6 concentration of 10^6 copies/mL and varying initial PFOA concentrations (0.1 mg/l, 10 mg/l, and 100 mg/l) are shown in Fig. 2 for the pure A6 culture and in Fig. 3 for the A6 enrichment culture. NH_4^+ oxidization during the Feammox process showed considerable variation among experiments. Several of these incubations were done sequentially, using cultures obtained at different times, which usually have differences in their activity. Furthermore, factors such as pH affect the activity of A6, with an optimal pH = 4 (Huang and Jaffé, 2018) which gradually increases as the reaction depicted in Eq. 1 progresses, all of which explains variability between experiments. In general, we see that in these Feammox incubations, only about 40% of the NH_4^+

in solution was oxidized over 100 days in the incubations with the pure A6 culture. In contrast, in the A6 enrichment culture incubations, as much as 50% of NH_4^+ was oxidized over the same time period (Fig. 3). In all incubations, the rate of ammonium oxidation decreases towards the end of the incubation period, even though the NH_4^+ concentration was still relatively high. This slow-down in the Feammox activity over time can be attributed to several factors, such as the depletion of CO_2 in the headspace, increase of pH, and buildup of Fe(II) and possibly NO_2^-. The incubations with the partial replacement of the spent Feammox medium (Experiment 3) were done to ameliorate these effects and extend the duration of the Feammox reaction.

The concentrations of PFOA over the incubation time for the various incubations are shown in Figs. 2b and 3b. While the fraction of PFOA degraded was relatively similar for the different initial PFOA concentrations, they diverged for larger incubation times (>20 days). Hence, since the variables that affect the Feammox process (i.e., NH_4^+, Fe(II), pH, etc.) change over time differently for different incubations, depending on the activity of the bacterial culture, the PFOA defluorination rate was determined for the various incubations over the first 7 days while values for the variables affecting the Feammox process remained relatively close. Results of this initial PFOA degradation rate vs. initial PFOA concentration are shown in Figure 4 and reveal a linear relationship between PFOA concentration and the PFOA degradation rate, which suggests a first-order biodegradation kinetics with respect to the PFOA concentration.

More PFAS degradation was observed in the A6 enrichment culture incubations vs. pure A6 culture incubations. As mentioned above, it was hypothesized that A6 can break a C-F bond, after which other heterotrophic organisms in the enrichment culture can break that partially defluorinated C-C bond. This in turn facilitates A6 to defluorinate the next shorter carbon chain PFAA intermediate that is formed, resulting in an overall increased defluorination rate. One

would expect, as will be confirmed below, that this will result in more PFOA degraded per NH_4^+ oxidized or higher f_{PFOA} values for the A6 enrichment culture than for the pure A6 culture, and possibly also differences in the relationship between the PFOA defluorination rate and the A6 biomass.

The production of F^- during these incubations is shown in Figs. 2c and 3c for the pure and enrichment culture incubations, respectively. 16S, a surrogate for A6 numbers, ranged from 3.31-3.57x10^6 copies/mL in A6 pure culture and 4.05-5.03x10^6 copies/mL in A6 enrichment culture, regardless of the PFOA concentration.

3.1.2 Feammox Activity and PFOA Degradation as a Function of the A6 Numbers (Experiment 2)

In both, the pure A6 culture incubations and the A6 enrichment culture incubations, the amount of NH_4^+ oxidized increased monotonically with increasing initial A6 concentration as shown in Figure S1a and Figure S2a, respectively. While for many biological kinetics the rates are linearly related to the biomass, this is clearly not the case for the Feammox reaction. This effect is most likely due to limitations in the transfer of the electrons to a solid-phase electron acceptor [Fe(III) in this case].

As is the case for NH_4^+ oxidized, the degradation of PFOA also increased monotonically with increasing initial A6 concentration as shown in Figure S1b and Figure S2b, respectively. Here there is again a noticeable difference in the effect of the biomass concentration on the PFOA degradation rate for the pure A6 culture incubations and the A6 enrichment culture incubations, the later one exhibiting more PFOA degradation over the same time period.

3.1.3 Feammox Activity and PFOA Degradation during the Replenish Experiment (Experiment 3)

Results of the replenishment incubations for the first 120 days of incubation are also shown in Figure 3. Comparing the PFOA degradation and F^- production of the replenish incubation, which had an initial PFOA concentration of 100 mg/l, to the single step batch incubation with the same initial PFOA concentration, revels that significantly more PFOA was degraded and F^- produced during the replenishment incubation. Accounting for the loss during the replenishment step, the amount of ammonium oxidized over the first 100 days in the replenishment incubation was 78.6 mg/L vs. 26.1 mg/L in the batch incubation. The corresponding PFOA degradation was 52.0 mg/L vs. 32.9 mg/L, respectively. These results show that PFOA degradation can be enhanced when more NH_4^+ is oxidized, aided by the removal of Feammox degradation products like Fe(II) and maintaining the pH closer to optimal.

3.2 Kinetic Model Calibration and Simulations

The experimental results show that A6 cultures, both pure and enrichment, grown at different times can have different levels of activity (e.g., rate of NH_4^+ oxidation, and hence growth). That difference is attributed to differences in the culture pH, Eh, and most importantly the age of the culture. Hence, we do not expect that the Feammox parameters will remain constant between experiments conducted with different batches of A6, and that the Feammox parameters for the incubations using different batches of A6 will need separate calibrations. We hypothesize that while PFAS defluorination is also affected by the Feammox activity, the parameters linking defluorination to the Feammox process will remain relatively constant.

In the proposed model, A6 growth is proportional to the Feammox reaction rate as represented by f_{A6} in Eq. (6), neither of which is affected by the presence of PFAS at the concentrations studied (Huang and Jaffé, 2018).

3.2.1 Derivation of Exponents, m and n, Using Results from Experiment 2

The next step in the model calibration was to derive the m and n parameters used in Equations (2) and (4) as shown above, with 16S as a surrogate for A6 biomass. Since Experiment 2 had the same initial NH_4^+, Fe(III), and PFOA concentrations, but different initial A6 concentrations, results from these incubations were used to derive the m and n parameters using the initial 5-day degradation rate (dC_{NH4}/dt and dC_{PFOA}/dt) and the initial concentrations of NH_4^+, Fe(III), and PFOA with the assumption that these concentrations were relatively constant over the first 5 days). The fitted *m* values to the data shown in Figures S1 and S2 were 9.28 and 3.63 for the A6 pure and A6 enrichment cultures, respectively, and the corresponding *n* values were 11.94 and 9.62. The k_{NH4} values were higher in the pure culture ($2.5x10^{-6}$) than in the enrichment culture ($8.7x10^{-7}$) when the concentration is expressed in mg/L, t in hours, and biomass in million copies/mL). The f_{PFOA}, was much higher in the enrichment culture than in the pure culture (0.027 vs. 0.0079), indicating that as discussed above, synergistic interactions between A6 and other bacteria in the enrichment culture result in a faster PFAS degradation rate.

3.2.2 Calibration of the model Using Results from Experiment 1

Using the *m* and *n* values obtained in the previous step, the parameter values of k_{NH4}, k_{FeIII}, and f_{A6} were first obtained for the Feammox reactions without PFOA degradation by solving the Equations (2), (3), and (6) numerically and fitting the parameters k_{NH4}, k_{FeIII}, and f_{A6}, to the experimental data of Feammox without PFOA (Table 1). The simulated NH_4^+, Fe(II), and

A6 concentrations describe the experimental results well, as shown in Figure 5. The model was then calibrated for the coupled Feammox and PFOA degradation reaction to solve the full system of Equations (2-6) using the highest PFOA concentration (100 mg/L) in the Experiment 1 to ensure the most reliable F^- production measurements (Fig. 6). Although the k_{NH4}, k_{FeIII}, f_{A6} parameter values were obtained by fitting the model to incubations without PFOA and then with initial PFOA concentrations of 100 mg/L, they are remarkably similar (Table 1), indicating that PFOA did not affect the Feammox process, as was the case in Huang and Jaffé (2019). The higher f_F, and f_{PFOA} values obtained for the A6 enrichment culture vs. the A6 pure culture, suggest as discussed above, that there is a synergy between A6 and other bacteria that results in a larger amount of PFOA defluorinated and hence F^- produced in the A6 enrichment culture.

To determine the effects of PFOA defluorination on the reduction of Fe(III) in terms of NH_4^+ oxidized, the ratios (Fe(II) produced/NH_4^+ removed) in mass/volume were compared between the pure Feammox simulation and the coupled Feammox reaction with PFOA degradation for the model. The Fe(II)/NH_4^+ ratio at the end of the 100-day incubations in the absence of PFOA, which is also the ratio of k_{FEIII}/k_{NH4}, were 18.75 (6.05, molar ratio) and 15.98 (5.51, molar ratio) for the A6 pure and A6 enrichment cultures, respectively (Table 1). These values are close to the k_{FEIII}/k_{NH4} 18.60 ratio (6, for a molar ratio) based on the stoichiometric relationship described in the Feammox reaction, for the A6 pure culture (Eq. 1). The lower k_{FEIII}/k_{NH4} value for the A6 enrichment culture might be due to the presence of NO_2^- in the enrichment culture reacting with the Fe(II) thus resulting in less measurable Fe(II).

Although the effect of defluorination on Fe(III) reduction is not modeled, we see similar trends in these experiments as that of Huang and Jaffe 2019 in the high PFAS concentrations, mainly that defluorination decreases the amount of Fe(III) reduced. Specifically our results show

that after PFOA was added at an initial concentration of 100 mg/L, the simulated average Fe(II)/NH_4^+ ratios between pure A6 and A6 enrichment culture were 14.17 (4.54 molar ratio) and 10.50 (3.39 molar ratio), respectively, where the decrease in the Fe(II)/NH_4^+ ratio from the Feammox process in the absence of PFOA indicates that some electrons were utilized for the reductive defluorination of PFOA as reported by Huang and Jaffé (2019). However, the substantially lower Fe(II)/NH_4^+ ratio for the incubations with PFOA cannot be fully attributed to the effect of defluorination, suggesting that some of the Fe(II) produced was oxidized to Fe(III) by the NO_2^- produced, or perhaps O_2 contamination while sacrificing the vials. The effect of defluorination by A6 on the amount of Fe(III) reduced is not measurable for incubations with the lower PFAS concentrations used in this effort, and much less with PFAS concentrations that are typical for most environmental settings, therefore the effect of defluorination of Fe(III) reduction was not included in the model formulation.

As already discussed above, during the 100-day incubations, almost twice as much PFOA was degraded in the incubations with the A6 enrichment culture than in the incubations with the pure A6 culture (57% vs. 31%). During the same period, 49% of NH_4^+ was oxidized in the pure A6 pure, whereas 57% of NH_4^+ was oxidized in the A6 enrichment culture. Hence, these results also indicate that in the A6 enrichment culture incubations, more PFOA is degraded per amount of NH_4^+ oxidized than in the pure A6 culture incubations, again, indicating a synergy between A6 and other bacteria present in the enrichment culture. This is reflected in the higher values of f_{PFOA} for the A6 enrichment culture vs. that for the pure A6 culture, as shown in Table 1.

3.2.3 Model Evaluation with testing datasets

After being calibrated using the data from Experiment 1 at 100 mg/L initial PFOA concentration, the model was evaluated using the datasets from the experiments at different

initial PFAS concentrations that were not used for the calibration (Fig. 1). The model, using the derived model parameters, was able to describe the Feammox and PFAS degradation dynamics at initial PFOA concentration of 0.1 mg/L (Fig. 7), showing that similar percentages of PFOA removal from the cultures were simulated at high and low initial PFOA concentrations, which agrees with Huang and Jaffé (2019) as shown in Figure 6 and Figure 7. The exception was that a significant discrepancy between the simulated and observed F^- in solution (Fig. 7) was observed, which is attributed partially due to analytical limitations at the lower F^- concentrations (Jaffé et al., 2021), and which is the reason incubations were done at the rather high concentrations of 100 mg/L PFOA, where the produced F^- could be monitored more accurately. The measured and simulated dynamics, using the parameters obtained via calibration for the incubations with 100 mg/l PFOA, of incubations with PFOA with an initial concentration of 10 mg/L are shown in Figure S4, indicating that the model captures the A6 enrichment culture dynamics reasonably well.

It is interesting to note that in all the experiments shown here, as well as previous Feammox incubations with A6, the reaction slows down after two to three weeks. This can be due to a variety of factors such as limited nutrients (including NH_4^+, Fe(III), CO_2), buildup of reaction products (i.e., NO_2^-, Fe(II)), or an increase in pH. As seen from Equation 1, an increase in pH or buildup of Fe(II) will significantly affect the change in Gibbs free energy, potentially making the reaction unfavorable. Therefore, to determine if the PFAS defluorination and the Feammox reaction can be sustained for a longer period by maintaining consistent pH, NH_4^+, Fe (III) and CO_2 levels, and by removing Fe(II), the replenishment experiment (Experiment 3) discussed above was conducted, the results of the full 240 day-experiment are shown in Figure 8. The results show that a sustained nutrient input and more constant and optimal values of pH,

447 CO_2, and Fe(II), can prolong the Feammox reaction, resulting in the removal of 70% PFOA over
448 240 days, and the near complete defluorination of the PFOA removed, based on F^- produced.
449 Given that only a small fraction of volume was replaced at each step (~ 6.7%) there was Fe(II)
450 buildup over time, which may still have affected the reaction. Hence, under natural conditions,
451 where due to advection parameters such as pH, and Fe(II) remain relatively constant, one would
452 expect a more sustained degradation rate, socially over longer incubation periods. This also
453 indicates that the kinetic parameters presented here world be alerted if the model had been
454 calibrated to experiments that closer mimic natural conditions.

455 While F^- was modeled to link PFOA defluorination to F^- production for the incubations
456 with the high PFOA concentrations, it was not our goal to accurately model F^- as PFAS
457 intermediates were not measured, and under environmental conditions it is difficult to detect
458 changes in F^- concentrations due to defluorination, given the much lower PFAS concentrations
459 and background F^-. In previous experiments by Huang and Jaffe 2019, a fluorine (F) balance
460 showed that more than 80% of the total F present in the solution is present as in PFOA or as F^-
461 (Huang and Jaffé, 2019). Therefore, for this model we assume that as first order estimates, as
462 PFOA is degraded F^- is released at a ratio of 15 moles of F^- per 1 mole of PFOA. The close
463 agreement of the simulated and measured F^- concentrations for the 100 mg/L PFOA incubations
464 indicates that for these incubations the buildup if intermediates was negligible in terms of
465 fluorine content in the overall system.

466 ***3.2.6 Extension and Implications of the Model Results***

467 For environmental implication, we also simulated PFOA degradation by either
468 maintaining constant NH_4^+ and Fe(III) concentrations (57 mg/L and 837 mg/L, respectively),
469 representing a very large reservoir or resupply of these compounds, or by allowing their

concentrations to decrease with time during the Feammox process, which would be the case when these constituents are being utilized and not resupplied. As shown in Table 2, maintaining a high NH_4^+ and Fe(III) concentrations increased PFOA degradation over a one-year period by 65-126% for the A6 pure culture and by 22-48% for the A6 enrichment culture. Thus, in natural systems such as riverine sediments or wetlands where NH_4^+ and Fe(III) may be stable due to biomass turnover and sedimentation, PFOA degradation could be faster and less constraint by the availability of NH_4^+ and Fe(III) than in closed incubation systems, such as have been studied to date. Results also show that due to the non-linear relationship with the A6 biomass, increasing the A6 biomass 10-fold increases the increased PFOA degradation by only 12% in the pure A6 culture and by 24% in the A6 enrichment culture (Table 2).

To further test the kinetic model's applicability to other PFAS, PFOS degradation for initial PFOS concentrations of 0.1, 10, and 100 mg/L from Huang and Jaffé (2019) was simulated by assuming the same *m* and *n* parameters as determined for PFOA, since no experiments were conducted for different A6 initial concentrations for PFOS. Model parameters were determined by fitting the model, as described above, to the 100 mg/l PFOS incubations (Table 1), showing a good agreement between the fitted model output and experimental results (Fig. S5). Using these parameters, the model simulated the PFOS dynamics for initial concentrations of 0.1 and 10 mg/L (Fig. S6 and S7) with similar accuracy as that for PFOA, especially for the A6 enrichment culture. Furthermore, long-term simulation of PFOS degradation showed similar trends as PFOA (Table 2). Therefore, the proposed kinetic model coupling PFOA degradation with the Feammox process appears adequate in also simulating defluorination of other PFAAs.

4. Conclusions

A model formulation is presented, linking the oxidation of NH_4^+ and reduction of ferric iron (Feammox process) by Acidimicrobium Sp. A6 to the defluorination of PFOA and PFOS. The model was calibrated using a set of incubation data and tested against different incubations. Overall, the formulation captured the coupled Feammox dynamics and defluorination kinetics well.

The production of F^- was observed in all incubations with A6 activity where the concentration of PFAS decreased, indicating that these compounds were being defluorinated. Incubations were conducted with both, pure A6 cultures and with A6 enrichment cultures. Although the difference in NH_4^+ oxidation between these cultures was minor, there was significantly more PFAS defluorination in the enrichment culture per NH_4^+ oxidized than in the pure culture, indicating a synergism in the PFAS defluorination process between A6 and other organisms present. This is reflected in the model parameterization, where parameters obtained to describe the Feammox process are very similar for the pure A6 and A6 enrichment culture, while the parameters required to describe the PFAS changes vary substantially between the pure and enrichment culture.

The coupled modeling and experimental results show that the PFAS defluorination rate is proportional to the NH_4^+ oxidation rate, which makes sense given that NH_4^+ is the electron donor for both, the iron reduction ad PFAS defluorination. Results also show that the Feammox and defluorination kinetics increase monotonically but not linearly with the A6 biomass.

Although the parameters describing the Feammox reaction can vary depending on the specific activity of a culture, the model parameters linking the Feammox activity to

defluorination appear to be much less variable as shown in Table 1. The higher values of f_{PFOA}, f_F, for the A6 enrichment culture over the pure A6 culture shown in Table 1, also show that for both, PFOA and PFOS, significantly more defluorination per amount of NH_4^+ oxidized, and F^- production occurs in the enrichment culture incubations than in the pure culture incubations, and that these differences are consistent for PFOA and PFOS degradation.

The proposed model formulation will aid in the assessment of PFAS defluorination at PFAS contaminated sites where the Feammox process is occurring, and for the design and operation of potential A6-based PFAS bioremediation schemes.

Further studies on how the Feammox/PFAS defluorination kinetics are affected by various environmental conditions, including different Fe(III) phases and the presence of a much wider microbial community than in the enrichment cultures, as well as the presence of PFAS mixtures, are required to further refine the proposed model, and are under way.

Acknowledgements

Funding for this research was provided by SERDP project # ER20-1219. The replenishment experiment is part of a project that was funded by a grant from ExxonMobil.

References

Abhijith, G. R., Ostfeld, A. 2021. Model-based investigation of the formation, transmission, and health risk of perfluorooctanoic acid, a member of PFASs group, in drinking water distribution systems. Water Res. 204, 117626.

Ahmed, M. B., Alam, M. M., Zhou, J. L., Xu, B., Johir, M. A. H., Karmakar, A. K., Rahman, M. S., Hossen, J., Hasan, A. T. M. K., Moni, M. A. 2020. Advanced treatment technologies efficacies and mechanism of perand poly-fluoroalkyl substances removal from water. Proc. 25afety Environ. Protect. 136:1-14.

Allred, B. M., Lang, J. R., Barlaz, M. A., Field, J. A. 2015. Physical and biological release of poly- and perfluoroalkyl substances (PFASs) from municipal solid waste in anaerobic model landfill reactors. Environ. Sci. Technol. 49:7648-7656.

Beskoski, V.P., Yamamoto, A., Nakano, T., Yamamoto, K., Matsumura, C., Motegi, M., Beskoski, L.S., Inui, H., 2018. Defluorination of perfluoroalkyl acids is followed by production of monofluorinated fatty acids. Sci. Total Environ. 636, 355–359. https://doi.org/10.1016/j.scitotenv.2018.04.243.

Blotevogel. J., Giraud, R. J., Borch, T. 2018. Reductive defluorination of perfluorooctanoic acid by zero-valent iron and zinc: a DFT-based kinetic model. Chem. Engin. J. 335:248-254.

Bolan, N., Sarkar, B., Yan, Y., Li, Q., Wijesekara, H., Kannan, K., Tsang, D. C. W., Schauerte, M., Bosch, J., Noll, H., Ok, Y. S., Scheckel, K., Kumpiene, J., Gobindlal, K., Kah, M., Sperry, J., Kirkham, M. B., Wang, H., Tsang, Y. F., Hou, D., Rinklebe, J. 2021. Remediation of poly- and perfluoroalkyl substances (PFAS) contaminated soils – To mobilize or to immobilize or to degrade? J. Hazard. Materials. 401, 123892.

Buck, R. C., Franklin, J., Berger, U., Conder, J. M., Cousins, I. T., de Voogt, P., Jensen, A. A., Kannan, K., Mabury, S., van Leeuwen, S. P. J. Perfluoroalkyl and Polyfluoroalkyl Substances in theEnvironment: Terminology, Classification, and Origins. Integr. Environ. Assess. Manage. 7:513-541.

Che, S., Jin, B., Liu, Z., Yu, Y., Liu, J., Men, Y. 2021. Structure-Specific Aerobic Defluorination of Short-Chain Fluorinated Carboxylic Acids by Activated Sludge Communities. Environ. Sci. Technol. Lett. 8:668-674.

Chetverikov, S.P., Sharipov, D.A., Korshunova, T.T., Loginov, O.N., 2017. Degradation of perfluorooctanyl sulfonate by strain pseudomonas plecoglossicida 2.4-D. Appl. Biochem. Microbiol. 53, 533–538. https://doi.org/10.1134/S0003683817050027.

Cornell, R. M.; Schwertmann, U. The Iron Oxides: Structure, Properties, Reactions, Occurrences, and Uses; John Wiley and Sons Ltd., 2003.

Ge, J., S. Huang, I. Han, P. R. Jaffé. 2019. Degradation of tetra- and trichloroethylene under iron reducing conditions by *Acidimicrobiaceae sp.* A6. Environ. Pollut. 247:248-255.

Hamid, H., Li, L. Y., Grace, J. R. 2018. Review of the fate and transformation of per- and polyfluoroalkyl sustances (PFASs) in landfills. Environ. Pollut. 235:74-84.

Huang, S., M. Sima, Y. Long, C. Messenger, and P.R. Jaffé, 2022. Degradation of Perfluorooctanoic Acid (PFOA) in Biosolids by Acidimicrobium sp. Strain A6. *J. of Hazardous Materials*, https://doi.org/10.1016/j.jhazmat.2021.127699.

Huang, S., Jaffé, P. R. 2019. Defluorination of perfluorooctanoic acid (PFOA) and perfluorooctane sulfonate (PFOS) by acidimicrobium sp. Strain A6. Environ. Sci. Technol. 53:11410-11419.

Huang, S., Jaffé, P. R. 2018. Isolation and characterization of an ammonium-oxidizing iron reducer: *Acidimicrobiaceae* sp. A6. PloS ONE 13(4): e0194007. https://doi.org/10.1371/journal.pone.0194007.

Huang, S., C. Chen, X. Peng, and P.R. Jaffé. 2016. Environmental Factors Affecting the Presence of *Acidimicrobiaceae* and Ammonium Removal under Iron-reducing Conditions in Soil Environments. *Soil Biology and Biochemistry*, Vol. 98, pp. 148-158, doi: 10.1016/j.soilbio.2016.04.012.

Jaffé, P.R., Huang, S., Sima, M., Ross, I., Liu, J. 2021. ER20-1219: Biotransformation and Potential Mineralization of PFOS, PFHxS, and PFOA by Acidimicrobiaceae sp. A6 under Iron Reducing Conditions. SERDP final Report, https://serdp-estcp.org/index.php//content/download/53927/529646/file/ER20-1219%20Final%20Report.pdf

Ji, J., Peng, L., Redina, M. M., Gao, T., Khan, A., Liu P., Li, X. 2021. Perfluorooctane sulfonate decreases the performance of a sequencing batch reactor system and changes the sludge microbial community. Chemosphere. 279, 130596.

Kool, J. B., Parker, J. C., van Genuchten, M. Th. 1987. Parameter estimation for unsaturated flow and transport models – A review. J. Hydrol. 91:255-293.

Kucharzyk, K. H., Darlington, R., Benotti, M., Deeb, R., Hawley, E. 2017. Novel treatment technologies for PFAS compounds: A critical review. J. Environ. Manage. 204:757-764.

Kwon, B.G., Lim, H., Na, S., Choi, B., Shin, D., Chung, S., 2014. Biodegradation of perfluorooctanesulfonate (PFOS) as an emerging contaminant. Chemosphere 109, 221–225. https://doi.org/10.1016/j.chemosphere.2014.01.072.

Liu, C., Liu, J. 2016. Aerobic biotransformation of polyfluoroalkyl phosphate esters (PAPs) in soil. Environ. Pollut. 212:230-237.

Liu, J., Avendano, S. M. 2013. Microbial degradation of polyfluoroalkyl chemicals in the environment: A review. Environ. International. 61:98-114.

Murray, A. M., Mailard, J., Jin, B., Broholm, M. M., Holliger, C., Rolle, M. 2019. A modeling approach integrating microbial activity, mass transfer, and geochemical processes to interpret biological assays: An example for PCE degradation in a multi-phase batch setup. Water Res. 160:484-496.

Naidu, R., Nadebaum, P., Fang, C., Cousins, I., Pennell, K., Conder, J., Newell, C. J., Longpre, D., Warner, S., Crosbie, N. D., Surapaneni, A., Bekele, D., Spiese, R., Bradshaw, T., Slee, D., Liu, Y., Qi, F., Mallavarapu, M., Duan, L., McLeod, L., Bowman, M., Richmond, B., Srivastava, P., Chadalavada, S., Umeh, A., Biswas, B., Barclay, A., Simon, J., Nathanail, P. 2020. Per- and poly-fluoroalkyl substances (PFAS): Current status and research needs. Environ. Technol. Innovation. 19, 100915.

Ruiz-Urigüen, M., W. Shuai, S. Huang, and P.R. Jaffé, "Biodegradation of PFOA in Microbial Electrolysis Cells by Acidimicrobiaceae sp. Strain A6," Chemosphere, 2022, https://doi.org/10.1016/j.chemosphere.2021.133506.

Shu, D., Y. He, H. Yue, and S. Yang. 2016. Effects of Fe(II) on microbial communities, nitrogen transformation pathways and iron cycling in the anammox process: kinetics, quantitative molecular mechanism and metagenomic analysis. RSC Adv., 2016, 6, 68005.

Senevirathna, S.T.M.L.D., Bal Krishna, K.C., Mahinroosta, R., Sathasivan, A. 2022. Comparative characterization of microbial communities that inhabit PFAS-rich contaminated sites: A case-control study. J. Hazardous Materials. 423, 126941.

Sima, M. W. and P. R. Jaffé, 2021. A Critical Review of Modeling Poly- and Perfluoroalkyl Substances (PFAS) in the Soil-Water Environment. Sci. Total Environ. 757, 143793.

J. Šimůnek, J., van Genuchten, M. Th., Šejna, M. 2012. HYDRUS: Model use, Calibration, and Validation. Trans. ASABE. 55:1261-1274.

Starzak, M. 1994. Macroapproach kinetics of ethanol fermentation by Saccharornyces cerevisiae: experimental studies and mathematical modelling. Chemical Engine. J. 54:221-240.

Teaf, C. M., Garber, M. M., covert, D. J., tuovila, B. J. 2019. Perfluorooctanoic acid (PFOA): environmental sources, chemistry, toxicology, and potential risks. Soil Sediment Contamin. 28:258-273.

United States Environmental Protection Agency (USEPA). 2020. Drinking Water Health Advisories for PFOA and PFOS. https://www.epa.gov/ground-water-and-drinking-water/drinking-water-health-advisories-pfoa-and-pfos (accessed 2, November 2021).

Yi, L.B., Chai, L.Y., Xie, Y., Peng, Q.J., Peng, Q.Z., 2016. Isolation, identification, and degradation performance of a PFOA-degrading strain. Genet. Med. Res. 15 https:// doi.org/10.4238/gmr.15028043 gmr.15028043.

668 Table 1. Calibrated parameters for PFOA and PFOS. The model was first calibrated with pure
669 Feammox process without PFAS to obtain the f_{A6} parameter. Assuming the f_{A6} parameter did not
670 change, other parameters were calibrated from Experiment 1 at 100 mg/L initial PFAS
671 concentrations. (Fig. 1).

672

PFAS	A6 Culture	k_{NH4}	k_{FeIII}	f_{A6}	f_{PFOA}	f_F	k_{FeIII}/k_{NH4} *(mass)*	k_{FeIII}/k_{NH4} *(mole)*
No PFAS (Feammox)	pure	3.96×10^{-7}	7.44×10^{-6}	0.1153	-	-	18.75	6.05
	enrichment	4.03×10^{-7}	6.43×10^{-6}	0.1403	-	-	15.98	5.15
PFOA	pure	4.59×10^{-7}	6.51×10^{-6}	0.1153	0.0119	0.2419	14.17	4.57
	enrichment	5.06×10^{-7}	5.32×10^{-6}	0.1403	0.0211	0.4536	10.50	3.39
PFOS	pure	3.02×10^{-7}	4.48×10^{-6}	0.1153	0.0095	0.1333	14.79	4.77
	enrichment	2.36×10^{-7}	2.93×10^{-6}	0.1403	0.0279	0.5461	12.41	4.00

673

674 Table 2. Simulated PFAS degradation under plausible natural conditions (at 0.1 mg/L initial
675 PFAS concentration) based on parameters derived from PFAS concentration of 100 mg/L in pure
676 A6 and A6 enrichment culture, respectively. NH_4^+ and Fe(III) were either maintained at constant
677 (57 and 837 mg/L, respectively) or decreased during the Feammox reaction without
678 replenishment of NH_4^+ and Fe(III).
679

PFAS	Culture	NH_4^+	Fe(III)	% of PFOA degraded in given months			
				3 mon	6 mon	9 mon	12 mon
PFOA	A6 x 1	No replenishment		25.1	33.2	37.1	39.2
	A6 x 1	Maintain at initial concentrations		41.5	67.8	82.8	91.1
	A6 enrichment x 1	No replenishment		52.7	65.5	70.7	73.3
	A6 enrichment x 1	Maintain at initial concentrations		78.2	97.1	99.7	>99.9
	A6 x 10	No replenishment		27.6	35.4	39.0	41.0
	A6 x 10	Maintain at initial concentrations		46.6	72.2	85.8	92.8
	A6 enrichment x 10	No replenishment		65.5	76.0	79.9	81.8
	A6 enrichment x 10	Maintain at initial concentrations		88.9	99.1	99.9	>99.9
PFOS	A6 x 1	No replenishment		18.4	26.0	30.0	32.5
	A6 x 1	Maintain at initial concentrations		28.0	49.8	65.7	76.9
	A6 enrichment x 1	No replenishment		44.3	61.4	69.5	74.0
	A6 enrichment x 1	Maintain at initial concentrations		58.2	86.1	96.0	>99.0
	A6 x 10	No replenishment		20.6	28.1	31.9	34.3
	A6 x 10	Maintain at initial concentrations		32.1	54.5	69.8	80.1
	A6 enrichment x 10	No replenishment		59.2	74.2	80.4	83.7
	A6 enrichment x 10	Maintain at initial concentrations		74.7	94.2	98.8	>99.0

Fig. 1. Model parameterization (calibration) and evaluation (testing). The 100 mg/L PFOA incubations from Experiment 1, were used for parameterization and the remaining incubations were used as testing datasets. The f_{A6} parameter was obtained by fitting the pure Feammox process and used for all experiments.

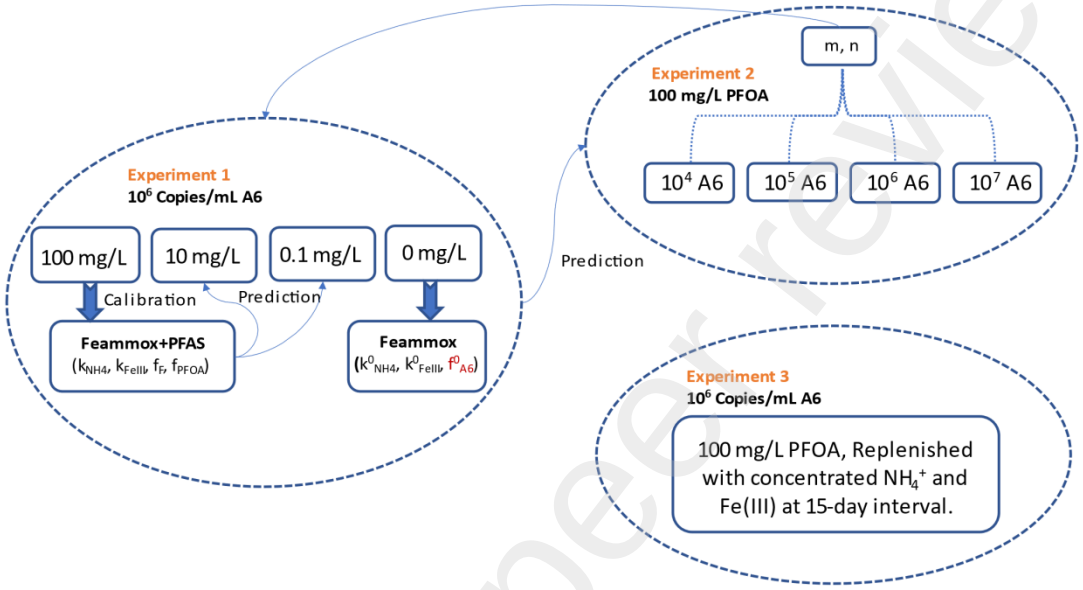

698 Fig. 2. NH_4^+ oxidation, PFOA biodegradation, and F^- production in pure A6 culture incubations
699 from Experiments 1 trough 3.

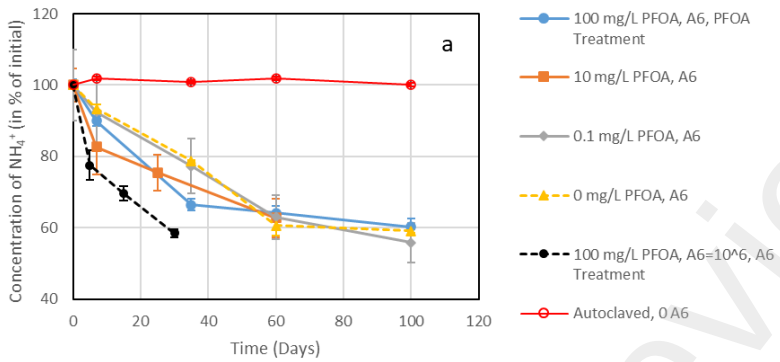

700

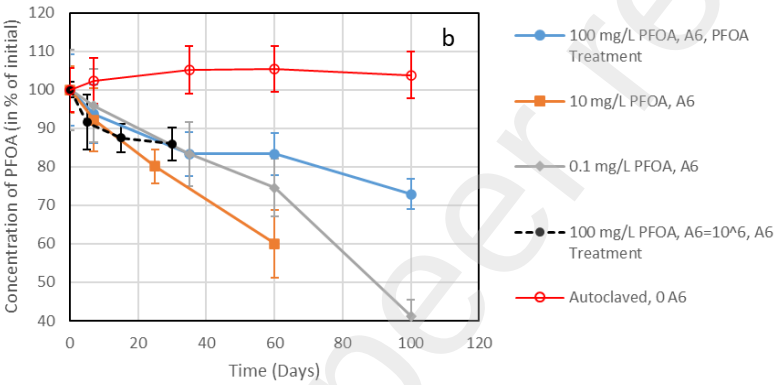

701

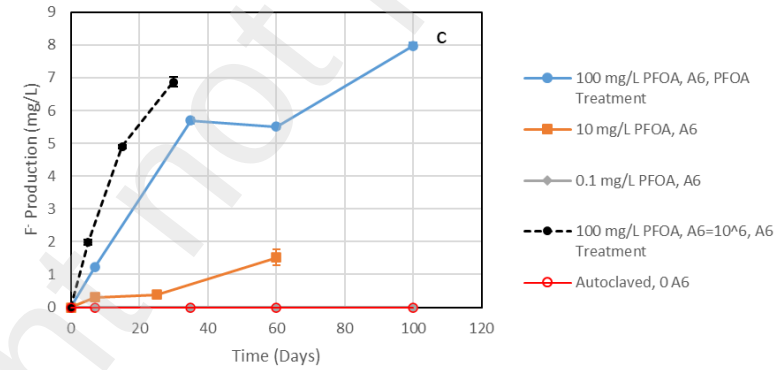

702

703 Fig. 3. NH_4^+ oxidation, PFOA biodegradation, and F^- production in A6 enrichment culture
704 incubations from Experiments 1 trough 3.

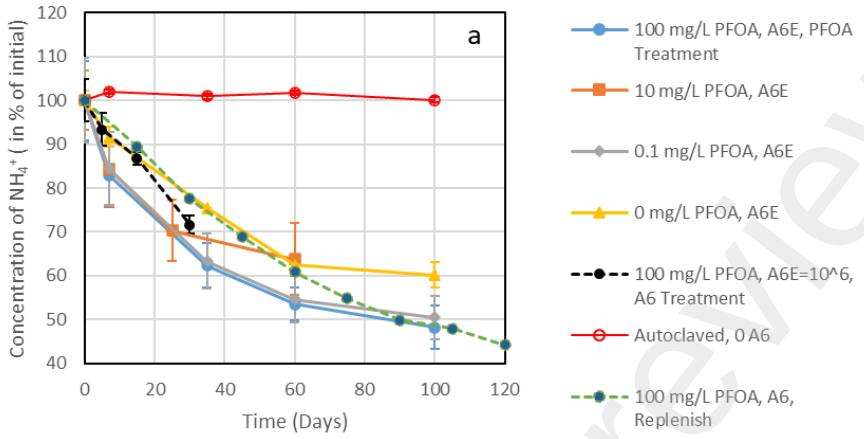

705

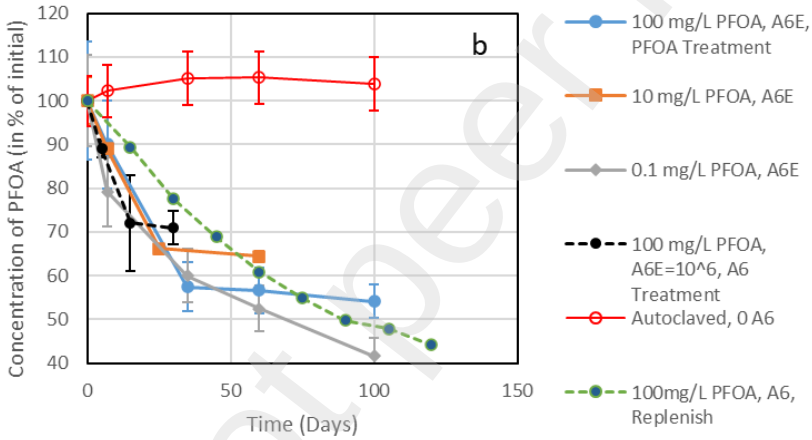

706

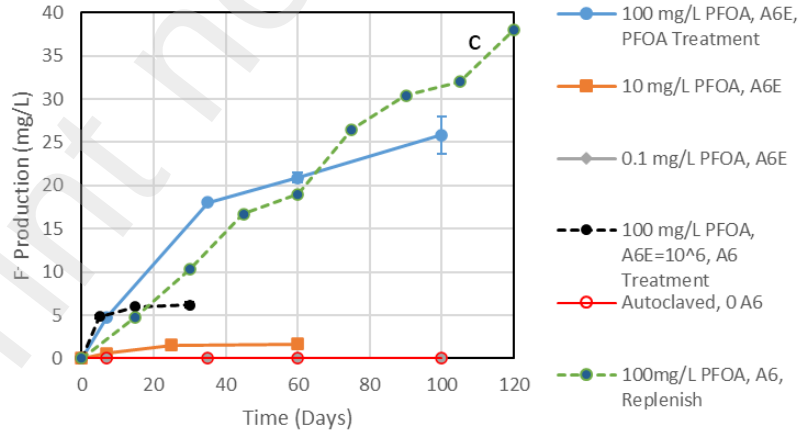

707

708 Fig. 4. Initial PFOA degradation rate (0-7 days) as a function of the initial PFOA concentrations
709 in Experiment 1.

710

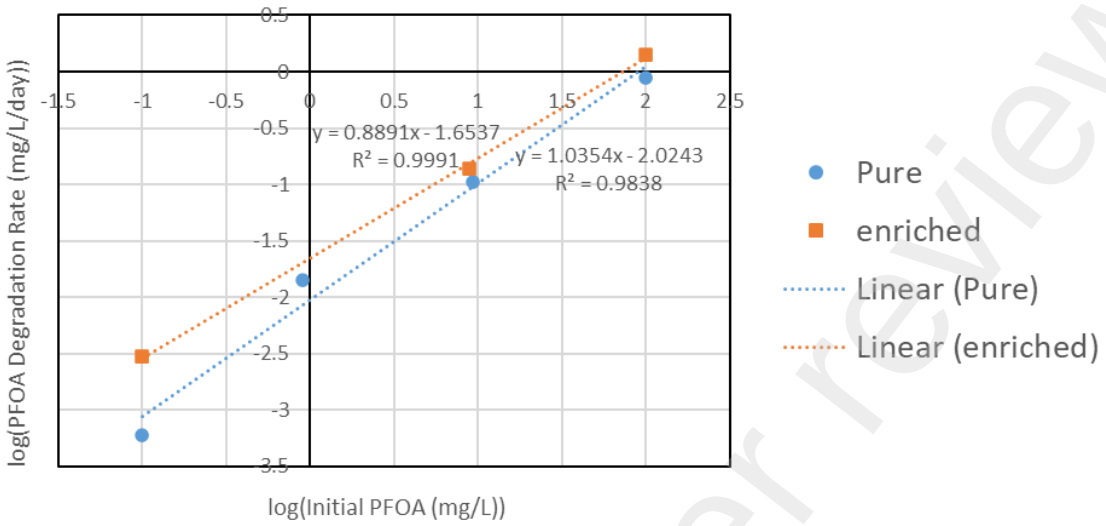

711

712 Fig. 5. Measured and simulated NH_4^+, Fe(II), and A6 concentrations vs. time during Feammox
713 reaction without PFOA in the pure A6 and A6 enrichment cultures (Table 1).

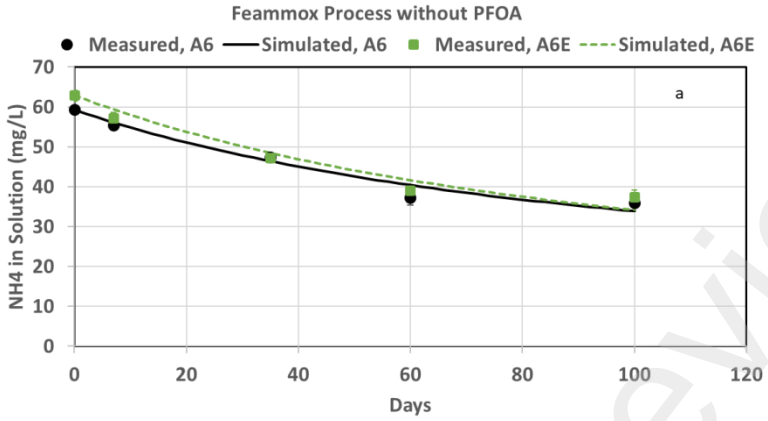

714

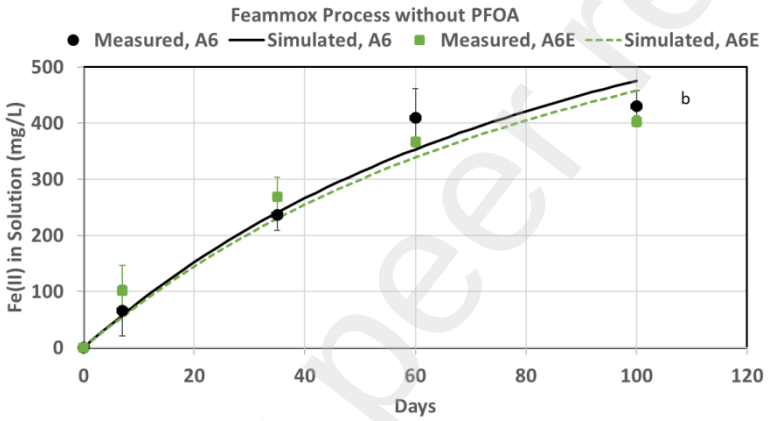

715

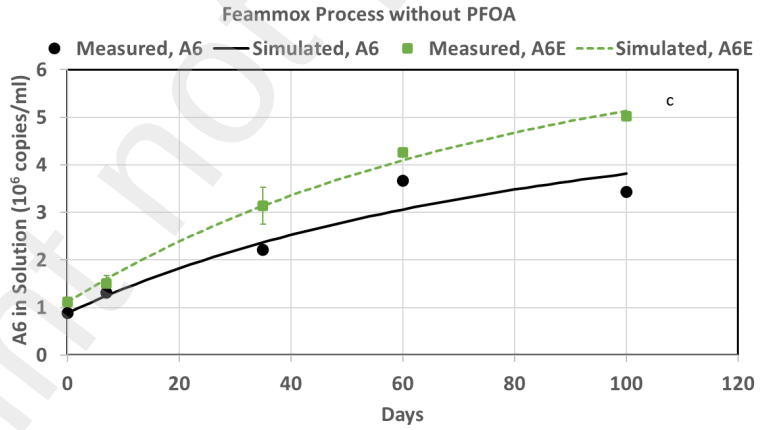

716
717
718
719

Fig. 6. Measured and simulated NH_4^+, Fe(II), PFOA, F^-, and A6 concentrations vs. time in pure A6 and enrichment cultures for the Experiment 1 for incubations with an initial PFOA concentration of 100 mg/L (Table 1).

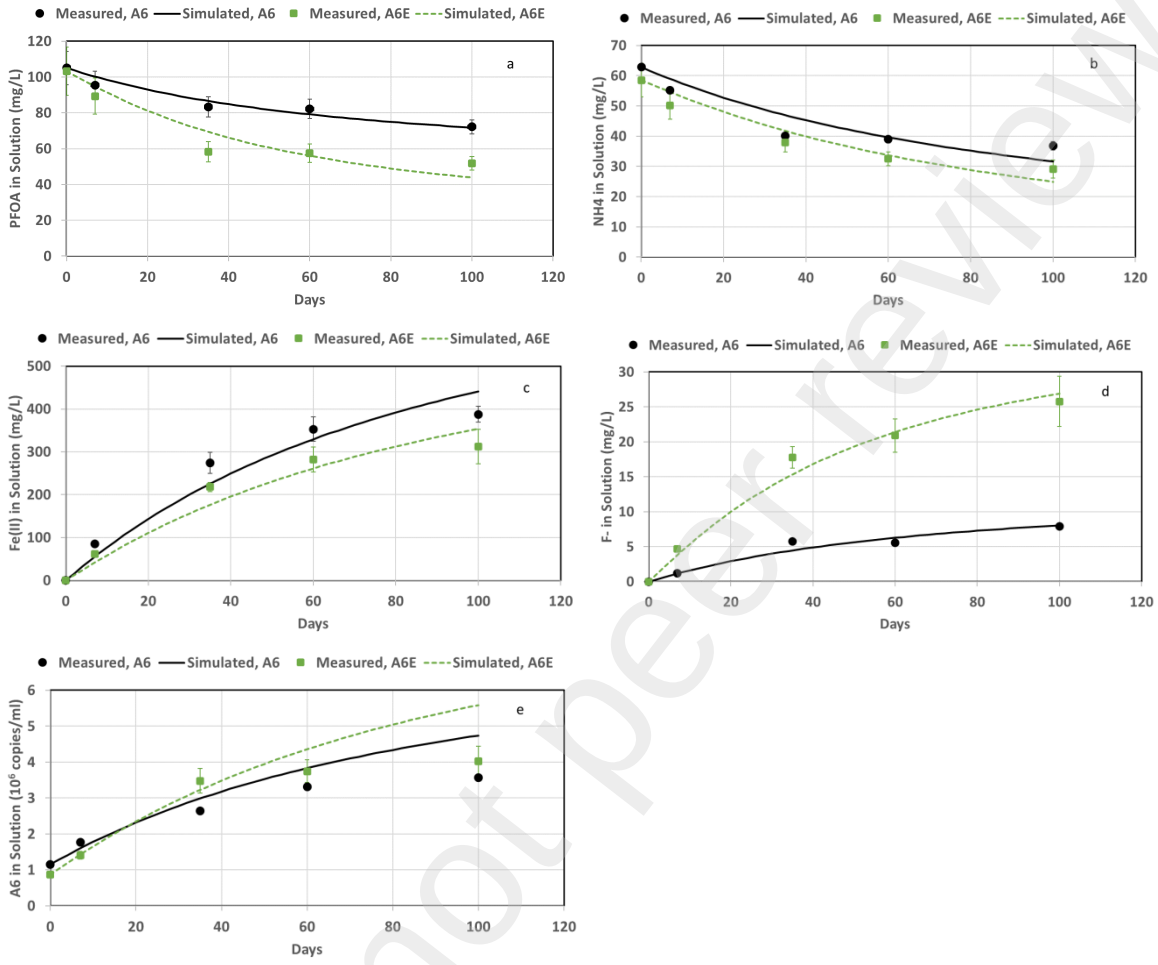

Fig. 7. Predicted NH_4^+, Fe(II), PFOA, F^-, and A6 concentrations with time in pure A6 and enrichment cultures for Experiment 1 incubations with an initial PFOA concentration of 0.1 mg/L , which was calibrated using the 100 mg/L concentration dataset (Table 1).

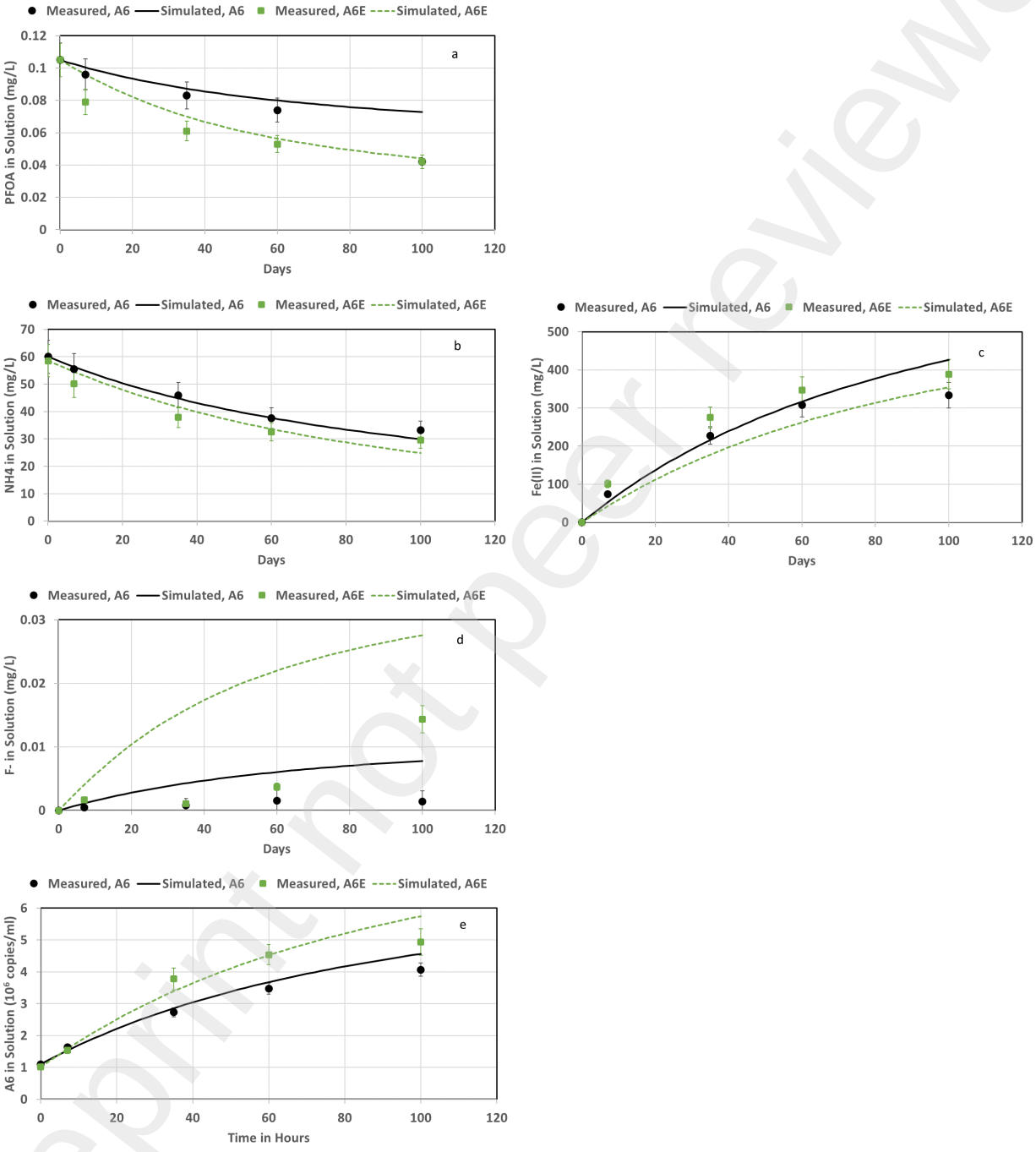

740

741 Fig. 8. Replenishment experiment results (Experiment 3) (Table 1).

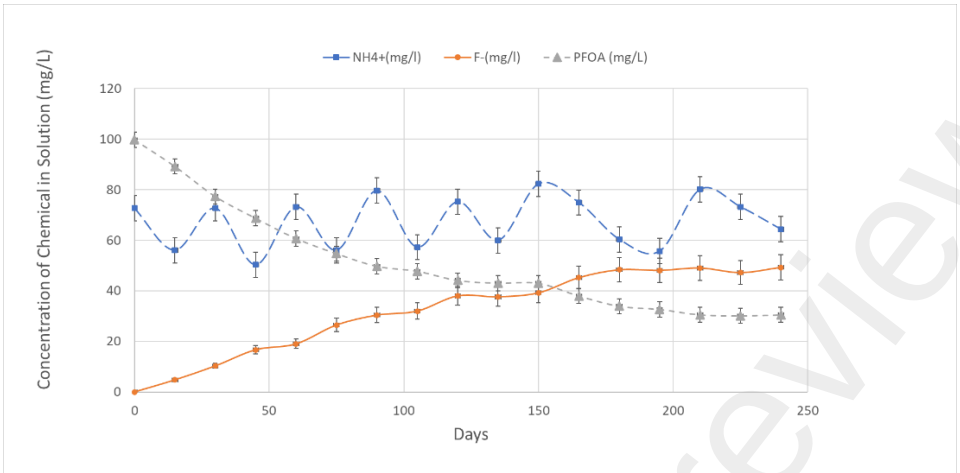

742

743 Supplemental Materials
744
745 Fig. S1. NH_4^+ oxidation, PFOA biodegradation, and F^- production in A6 pure cultures for
746 different initial A6 biomass concentrations from Experiment 2.
747

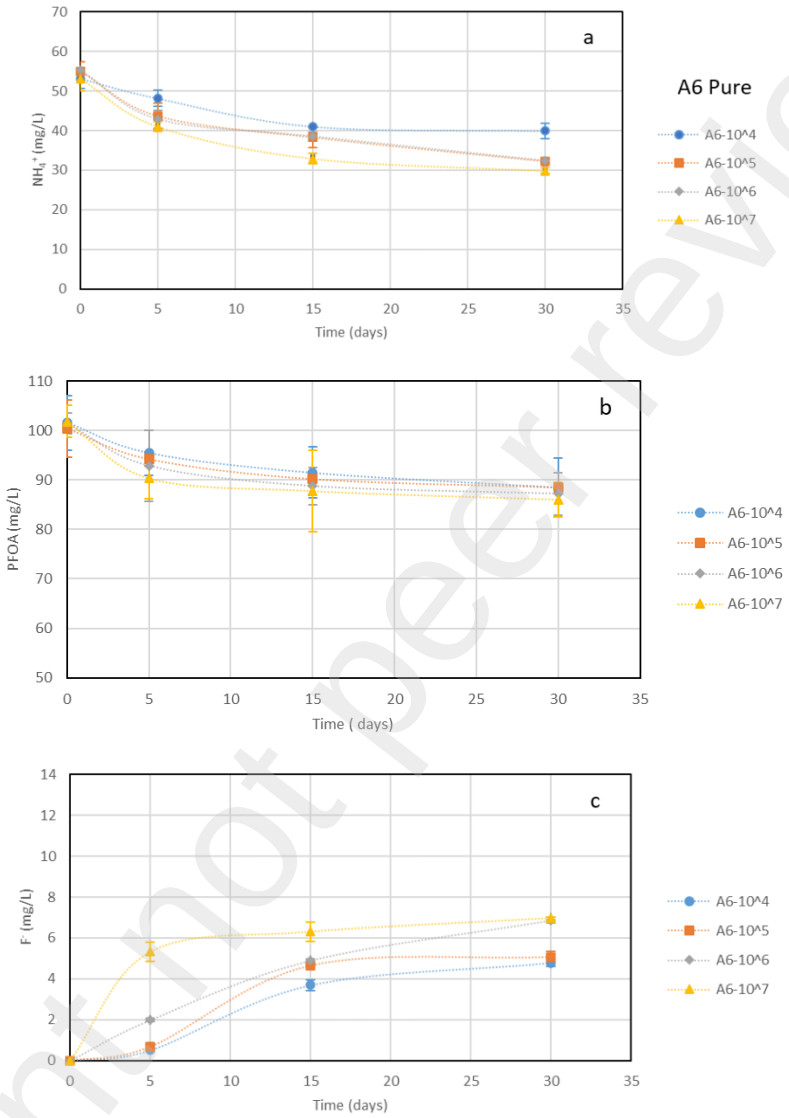

748
749
750
751

752 Fig. S2. NH_4^+ oxidation, PFOA biodegradation, and F^- production in A6 enrichment cultures for
753 different initial A6 biomass concentrations from Experiment 2.
754

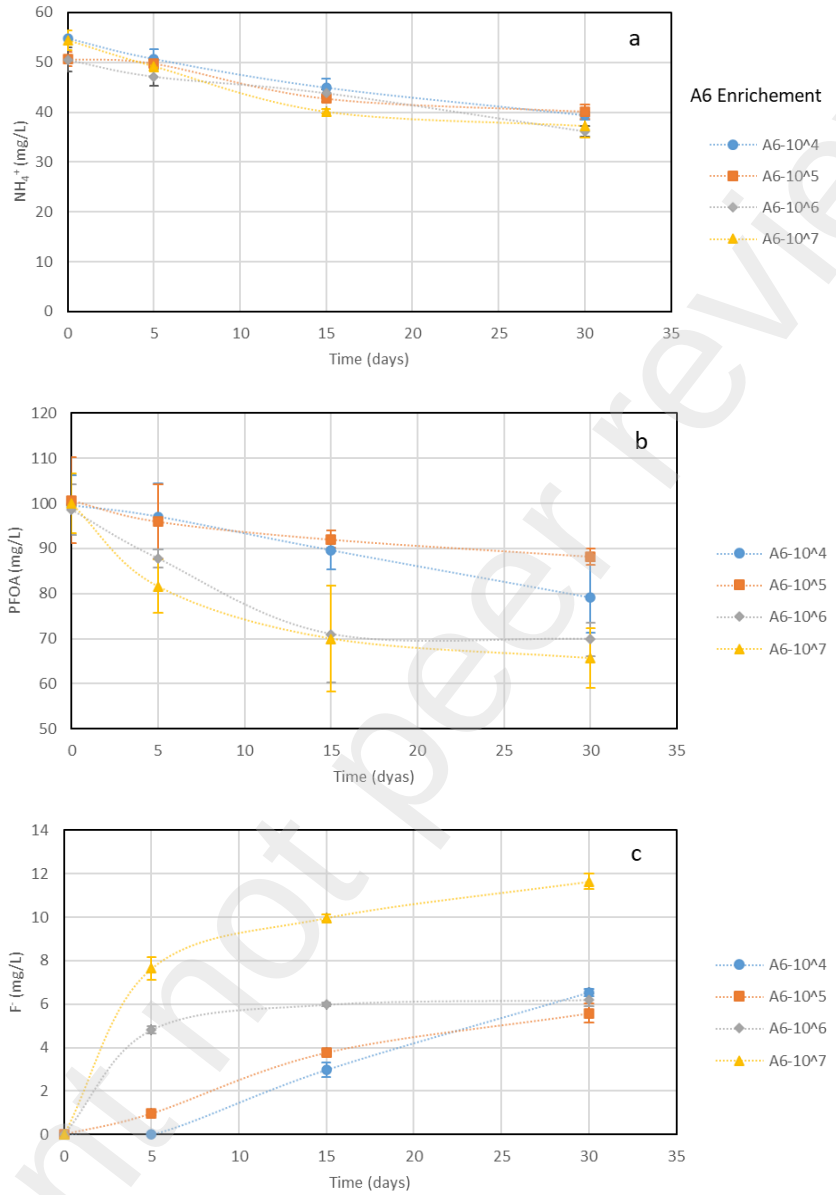

755

756

757
758

759

760 Fig. S3. Numerical algorithm to solve the system of kinetic equations.
761

762

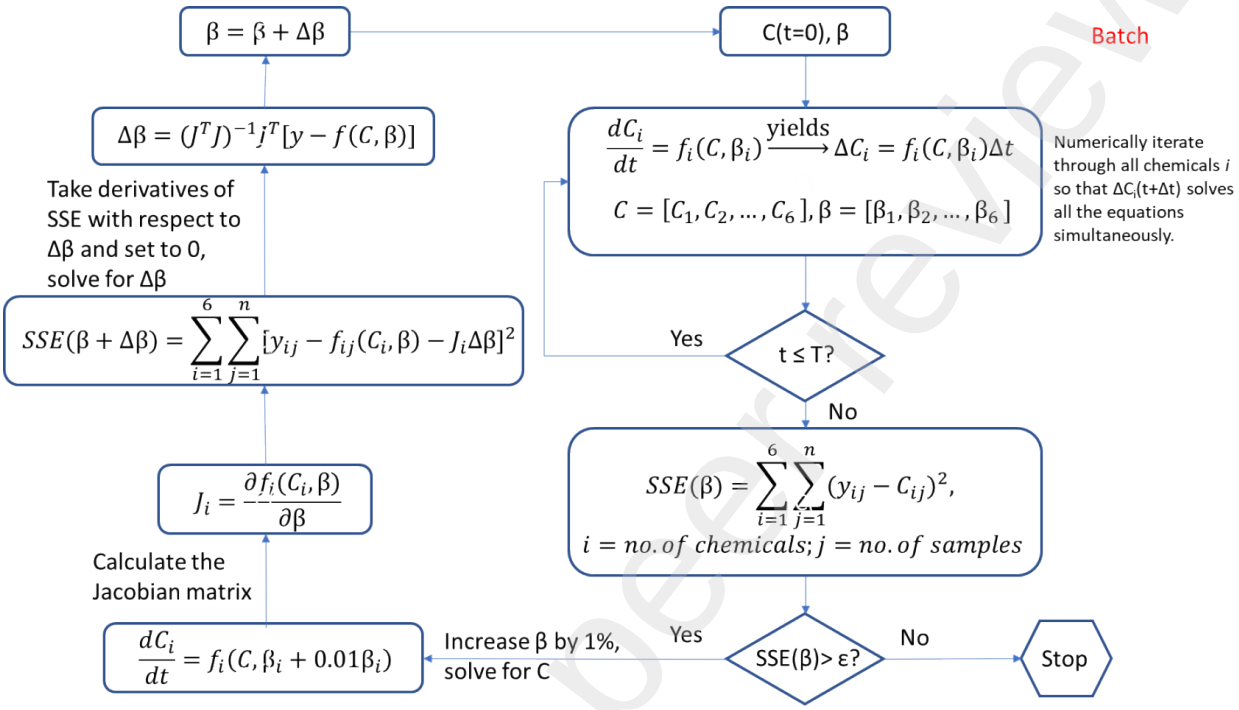

763

764 Fig. S4. Predicted Feammox process and PFOA degradation for an initial PFOA concentration of
765 10 mg/L. Parameters were calibrated from Experiment 1 and incubations with an initial PFOA
766 concentration of 100 mg/L (Table 1).

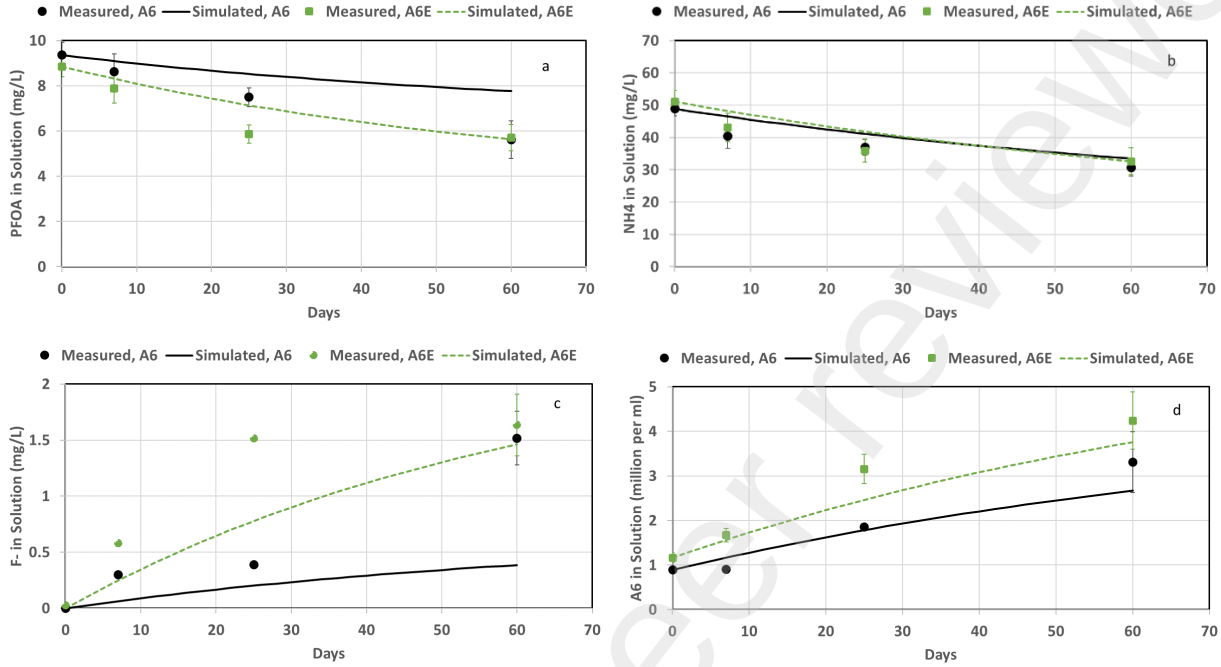

767

768

769

770

771 Fig. S5. Fitted NH_4^+, Fe(II), PFOS, F^-, and A6 concentrations vs. time for pure A6 and
772 enrichment culture incubations for PFOS at an initial concentration of 100 mg/L (Table 1).

773

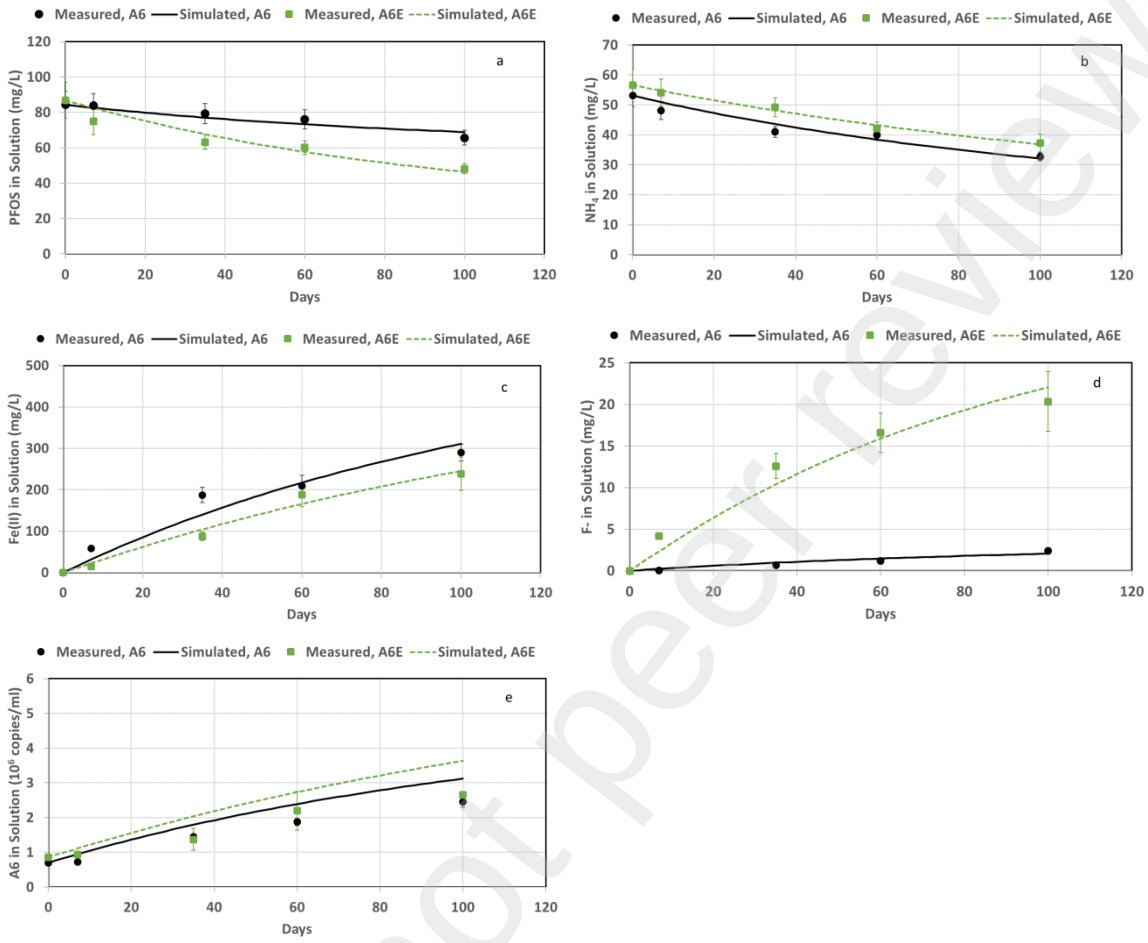

774

775

776

Fig. S6. Predicted NH_4^+, Fe(II), PFOS, F^-, and A6 concentrations vs time for pure A6 and enrichment culture incubations for the initial PFOS concentration of 0.1 mg/L using parameters calibrated from the 100 mg/L PFOS concentration (Table 1).

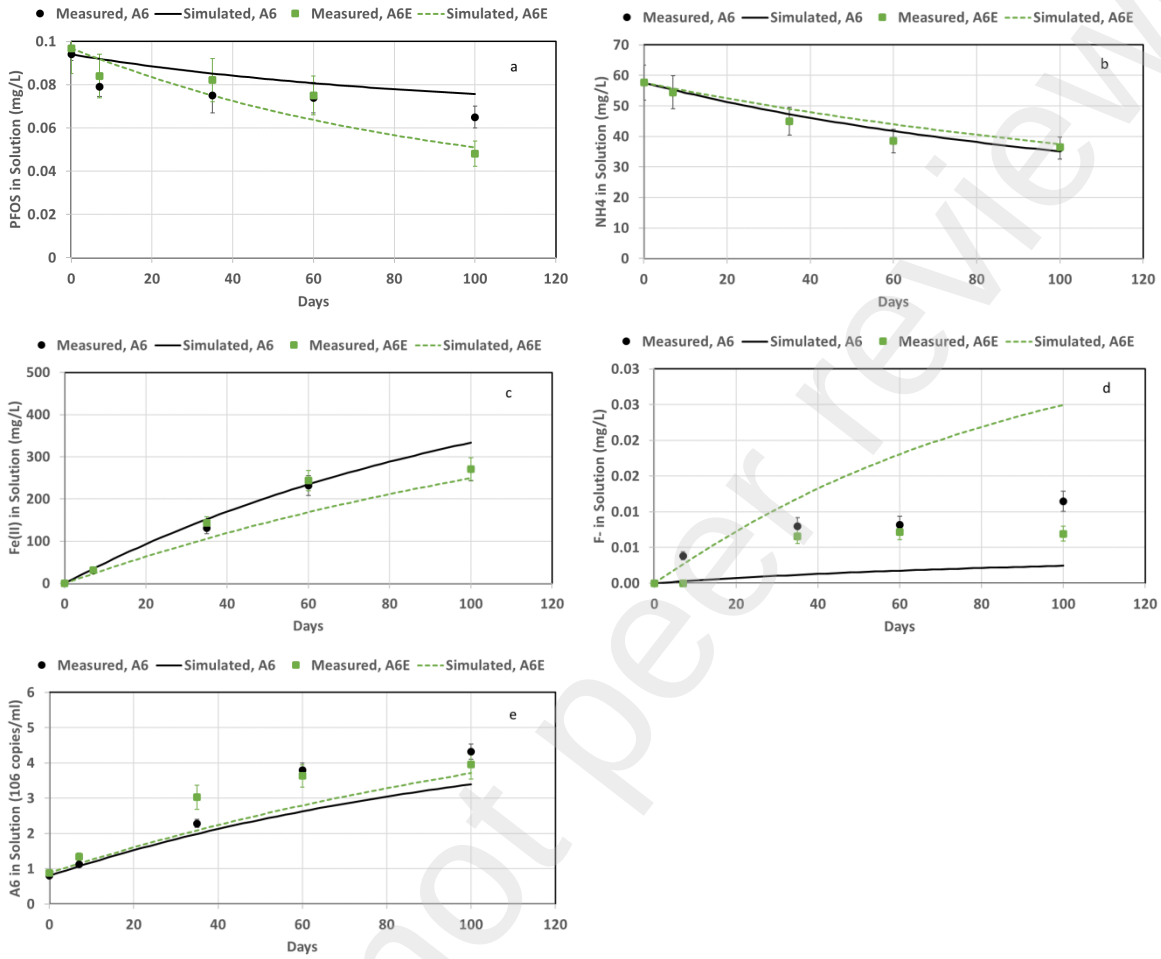

785 Fig. S7. Predicted Feammox process and PFOS degradation for the initial PFOS concentration of
786 10 mg/L using parameters calibrated from the 100 mg/L PFOS concentration (Table 1).
787

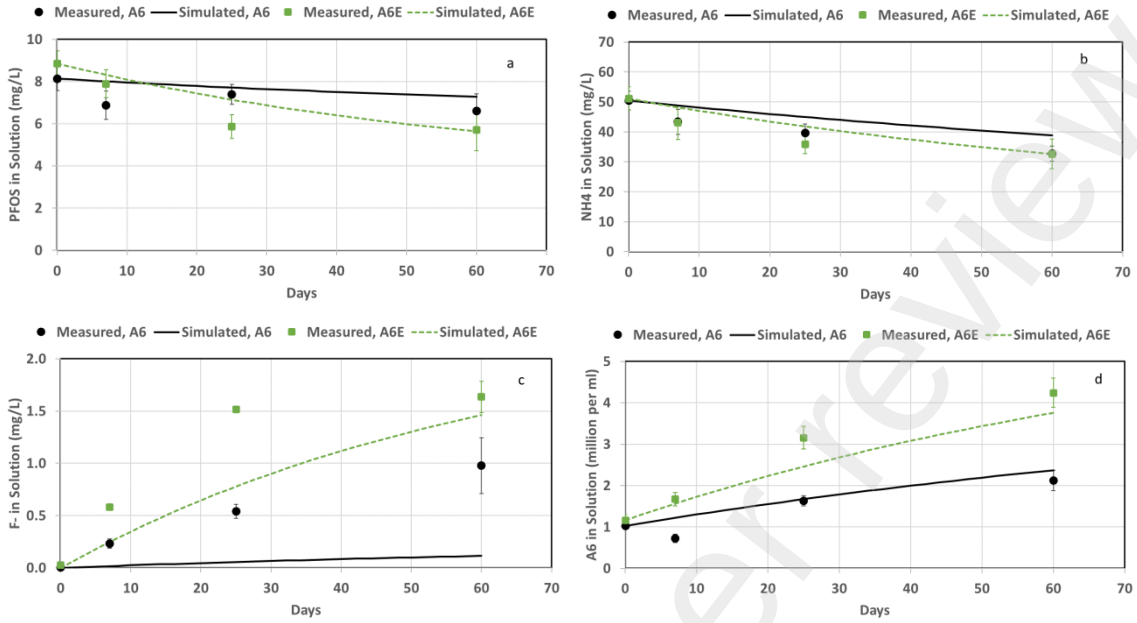

788
789
790
791
792